Delta resonance and nonlocal effects in pion photoproduction from nuclei

L. Tiator*
TRIUMF, Vancouver, British Columbia, Canada V6T 2A3

L. E. Wright
Physics Department, Ohio University, Athens, Ohio 45701
(Received 30 March 1984)

The photoproduction of charged pions from light nuclei is investigated in a distorted wave impulse approximation carried out in momentum space. This permits a straightforward inclusion of nonlocal terms in the pion production operator such as that of Blomqvist and Laget. The interaction of the outgoing pion with the residual nuclear state is described by the optical potential of Stricker, McManus, and Carr. The cross section for pion production from p-shell nuclei is decomposed into partial cross sections labeled by transition angular momenta and spin which are almost independent of nuclear structure. Using the reaction $^{13}C(\gamma,\pi^-)^{13}N_{g.s.}$, the effects of the delta isobar in the production operator on these partial cross sections is investigated. The same reaction is used to demonstrate the inadequacy of local coordinate space analyses.

I. INTRODUCTION

Due to a number of experimental improvements in recent years and better theoretical analyses,[1-3] the photoproduction of charged pions from nuclear targets holds the promise of becoming a major tool for investigating three aspects of nuclear and intermediate energy physics. These are pion production in the nuclear medium, nuclear matrix elements, and pion propagation in the nuclear medium. Of particular interest are pion production differential cross sections for cases where the final nucleus is in a definite final state. This final nuclear state is usually the ground state, but it can be some well-separated excited state. A number of such experiments on p-shell nuclei have been carried out in the past decade,[4-14] and increasing numbers of new experiments are being carried out or being planned at electron accelerator laboratories. In many cases the pions are produced not by real photons, but directly by electron beams, and virtual photon theory is used to extract the photoproduction cross section. The validity of virtual photon theory for pion production within 50 MeV of the end point from light targets has been investigated theoretically,[15] and been confirmed experimentally.[10]

Most of the experimental results obtained to date, particularly those near threshold, are in reasonable agreement with various theoretical calculations[2,16-22] which assume a distorted wave impulse approximation (DWIA) model for pion photoproduction from nuclei. In DWIA a photon penetrates the nucleus and interacts with a single bound nucleon resulting in the emission of a charged pion leaving the nucleon in some different shell model state. The interaction of the outgoing pion with the remaining nucleons in the nucleus is described by an optical potential which is obtained from fits to pion elastic scattering. There are three basic ingredients to a DWIA model: the pion production operator from a free nucleon, nuclear transition matrix elements, and the pion optical potential. The various theoretical works referenced above have used different forms of these three ingredients, and furthermore have made various approximations in carrying out their calculations. There are some cases[7] where the discrepancies between experiment and theory are large, but as stressed by Tabakin and co-workers,[2,17] it is important that all the ingredients of a DWIA analysis be handled as well as possible before drawing any final conclusion on the validity of DWIA. A major difficulty with applying the DWIA to pion photoproduction is that the pion production operator depends strongly on various momenta, and thus is a nonlocal operator in coordinate space.

In this paper we report on a new DWIA analysis of pion photoproduction from nuclei carried out in momentum space. Working in momentum space rather than coordinate space permits a straightforward treatment of all nonlocal effects arising from the production operator. Apart from the recent paper by Toker and Tabakin,[22] all previous DWIA analyses of pion photoproduction from nuclei have neglected portions of the momentum dependent terms in the production operator. Toker and Tabakin include all nonlocalities in a mixed coordinate-momentum space calculation, but at the cost of handling various terms somewhat differently and having to introduce phase shift equivalent "mock" pion wave functions which can more easily be smeared by the nonlocal propagators.

In Sec. II we give the formalism for calculating the pion production differential cross section in momentum space and in Sec. III we give a practical method for carrying out the Fourier transformation of the pion optical model wave function into momentum space. The plane wave impulse approximation (PWIA) is derived in Sec. IV and commonly used local approximations in coordinate space representation are discussed. We also show in Sec. V that in an LS-coupling scheme for the nuclear matrix elements of the p-shell, we can define partial cross sec-

tions which are characterized by the angular momentum (L), spin (S), and total spin (J) transferred to the nucleus. Furthermore, these partial cross sections are almost independent of nuclear structure and hence universal for all 1p-shell nuclei. In Sec. VI we specify in more detail the ingredients of our DWIA analysis which are very similar to those discussed in Singham and Tabakin[2] apart from our handling of the nuclear matrix elements and working in momentum space.

In the remaining sections we present our results by first comparing the partial cross sections evaluated with our full nonlocal calculation to investigate the importance of the nonlocal contributions. As an application we study the reaction $^{13}C(\gamma,\pi^-)^{13}N_{g.s.}$ and compare our calculations to some older[11] and some preliminary data[23] on this reaction. Finally, we examine the delta isobar contribution to pion production from a nucleon as compared to pion production from a nucleus and examine the role of the delta isobar in the various partial cross sections.

II. DIFFERENTIAL CROSS SECTION IN DWIA

Following the conventions of Bjorken and Drell,[24] the differential cross section for the reaction $\gamma+A\rightarrow\pi+A'$ is given by

$$\frac{d\sigma}{d\Omega_\pi^{\text{c.m.}}}=\frac{\alpha}{4\pi}\frac{q^{\text{c.m.}}}{k^{\text{c.m.}}}\frac{m_i m_f}{W^2}\frac{\mathcal{F}_{\text{c.m.}}}{2(2J_i+1)}\sum_{M_i,M_f,\lambda}|\langle J_f M_f,T_f N_f;\pi\,|\,T\,|\,J_i M_i,T_i N_i;\gamma\rangle|^2\,, \tag{1}$$

where all kinematical quantities are given in the center of momentum frame (c.m.). The four-momenta of the photon and pion are denoted by $(E_\gamma,\vec{k})$ and $(E_\pi,\vec{q})$, respectively. The masses of the initial and final state nuclei are m_i and m_f, the total spins and spin projections are J_i,M_i and J_f,M_f, and the isospin and isospin projections are T_i,N_i and T_f,N_f. To correct for the lack of translation invariance of the shell model, the cross section is multiplied by the factor

$$\mathcal{F}_{\text{c.m.}}=\exp[b^2(\vec{k}-\vec{q})^2/2A]\,,$$

where b is the harmonic oscillator parameter and A the nuclear mass number. W is the total energy in the c.m. system, λ is the photon polarization, and α is the fine structure constant. The Jacobian which transforms the c.m. cross section into the laboratory frame can be written

$$\frac{d\Omega^{\text{c.m.}}}{d\Omega^{\text{lab}}}=\frac{Wq_{\text{lab}}^2}{q^{\text{c.m.}}[q_{\text{lab}}(k_{\text{lab}}+m_i)-E_\pi^{\text{lab}}k_{\text{lab}}\cos\theta_\pi^{\text{lab}}]}\,, \tag{2}$$

which for the most applications involving p-shell nuclei will differ from unity by less than 10%. In Fig. 1 we show the situation in the laboratory frame and introduce an important quantity, the momentum transfer $\vec{Q}=\vec{k}-\vec{q}$ which equals the final nuclear momentum $\vec{P}_f$.

In the DWIA, the nuclear pion production operator is a one-body operator so that

$$T=\sum_{\alpha,\alpha'}\langle\alpha'\,|\,t\,|\,\alpha\rangle C_{\alpha'}^\dagger C_\alpha\,,$$

where $C_{\alpha'}^\dagger$ and C_α are particle and hole creation and annihilation operators. Using the conventions of Ref. 25,

$$C_\alpha=\theta(\epsilon_a-\epsilon_F)a_\alpha+\theta(\epsilon_F-\epsilon_a)S_\alpha b_{-\alpha}^\dagger \tag{3}$$

where a_α is the particle destruction operator for energies ϵ_a above the Fermi energy ϵ_F and $b_{-\alpha}^\dagger$ is the hole creation operator for energies below the Fermi energy. Here α denotes a set of quantum numbers for orbit, spin, and isospin of a single particle, $\alpha=\{am;1/2m_\tau\}$ where $a=\{nlj\}$. The phase $S_\alpha=(-1)^{j-m}(-1)^{(1/2)-m_\tau}$ is necessary to maintain the transformation properties of the irreducible tensors.

Evaluating the nuclear matrix elements for Eq. (1) we obtain

$$\langle J_f M_f,T_f N_f;\pi\,|\,T\,|\,J_i M_i,T_i N_i;\gamma\rangle=\sum_{\alpha\alpha'}\langle J_f M_f,T_f N_f\,|\,C_{\alpha'}^\dagger C_\alpha\,|\,J_i M_i,T_i N_i\rangle\langle\alpha';\pi\,|\,t\,|\,\alpha;\gamma\rangle\,. \tag{4}$$

In Eq. (4) the nuclear structure and pion production dynamics are already separated, but in principle we have to sum over complete sets of single particle states α and α'. In practice this is not possible and we restrict α and α'

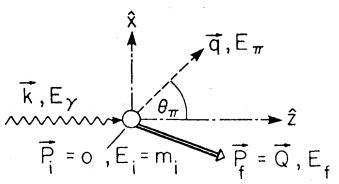

FIG. 1. Kinematics in the laboratory frame.

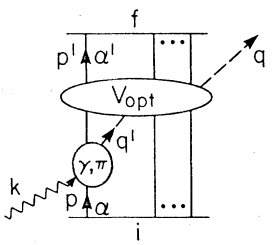

FIG. 2. Diagrammatic illustration of the DWIA process in momentum space. The momenta $\vec{p}$ and $\vec{q}\,'$ are integration variables, while $\vec{p}\,'=\vec{k}+\vec{p}-\vec{q}\,'$ is fixed by momentum conservation.

to the outermost shell. In this work we consider the p-shell nuclei from lithium through oxygen where the restriction to an open $1p$-shell and a closed $1s$-shell core has been very successful for nuclear structure and describes form factors adequately for momentum transfers up to about 2 fm^{-1}. That is, we get all the necessary nuclear structure information for nuclear ground states and some low lying excited states from admixtures of $1p_{3/2}$ and $1p_{1/2}$ nucleons.

The nuclear structure will be specified in the form of the double reduced one-body density matrix,

$$\Psi_{J;T}(a'a)=\hat{J}^{-1}\hat{T}^{-1}\langle J_f;T_f\|[C^{\dagger}_{a'}\times\tilde{C}_a]_{J;T}\|J_i;T_i\rangle \ , \tag{5}$$

where $\hat{x}\equiv\sqrt{2x+1}$, $\tilde{C}_\alpha=S_\alpha C_{-\alpha}$, and J and T are the total spin and isospin transferred to the nucleus in the transition. For the p shell, these are $J=0,1,2,3$ and $T=0,1$. Because of the negative parity of p-shell nucleons we find that the electric multipoles $E0$ and $E2$ and the magnetic multipoles $M1$ and $M3$ can contribute to both isoscalar and isovector transitions. However, since we only consider charged pion production, the isoscalar multipoles will not enter. For p-shell nuclei undergoing isovector transitions there are ten independent nuclear matrix elements which can be taken to be real without any further approximation. One source of these numbers are shell model calculations such as those of Cohen and Kurath,[26] while another possibility is to use a phenomenological method in which the nuclear matrix elements are constrained by experimental information.[20,27] Using the definition of Eq. (5), the nuclear part of the transition matrix element in Eq. (4) can be written as

$$\begin{aligned}&\langle J_fM_f;T_fN_f\,|\,C^{\dagger}_{\alpha'}C_\alpha\,|\,J_iM_i;T_iN_i\rangle\\&\quad=\sum_{\substack{J,M\\T,N}}(-1)^{j-m+(1/2)-m_\tau+J_i-M_i+T_i-N_i}\\&\qquad\times\hat{J}^2\hat{T}^2\begin{bmatrix}J_f & J_i & J\\ -M_f & M_i & M\end{bmatrix}\begin{bmatrix}T_f & T_i & T\\ -N_f & N_i & N\end{bmatrix}\begin{bmatrix}j' & j & J\\ -m' & m & M\end{bmatrix}\begin{bmatrix}\frac{1}{2} & \frac{1}{2} & T\\ -m'_\tau & m_\tau & N\end{bmatrix}\Psi_{J;T}(a'a)\ .\end{aligned} \tag{6}$$

The dynamics of pion photoproduction in DWIA is included in the single particle matrix element $\langle\alpha';\pi\,|\,t\,|\,\alpha;\gamma\rangle$ of Eq. (4). The elementary pion production operator has the general form

$$t=(L+i\vec{\sigma}\cdot\vec{K})\frac{\tau_{-\beta}}{\sqrt{2}}=\sum_{S,m_S}i^S(-1)^{m_S}\sigma^S_{-m_S}K^S_{m_S}\frac{\tau_{-\beta}}{\sqrt{2}}\ , \tag{7}$$

where $\sigma^0\equiv1$ and $K^0\equiv L$. For charged pion production t is pure isovector and $\beta=\pm1$ for $\pi^\pm$. The operators L and K depend on β, the photon polarization λ, and the four-momenta of the nucleons, pion, and photon. A general representation of the single particle matrix element which is valid for any pion production operator based on diagrammatic techniques can be given in momentum space (see Fig. 2).

$$\langle\alpha';\pi\,|\,t\,|\,\alpha;\gamma\rangle=\int d^3p\,d^3q'\Psi^*_{\alpha'}(\vec{p}\,')\phi^{(-)*}_\pi(\vec{q}\,',\vec{q})t_{\gamma,\pi}(\vec{p},\vec{p}\,',\vec{k},\vec{q}\,')\Psi_\alpha(\vec{p})\ , \tag{8}$$

where $\vec{p}\,'=\vec{p}+\vec{k}-\vec{q}\,'$ and Ψ_α is a single particle wave function which can be written as

$$\Psi_\alpha(\vec{p})=\sum_{m_lm_s}(lm_l\tfrac{1}{2}m_s\,|\,l\tfrac{1}{2}jm)\phi_{nlj}(p)Y^m_l(\hat{p})\chi_{m_s}\tau_{m_\tau} \tag{9}$$

with ϕ_{nlj} as the "radial" part of the wave function and χ,τ the Pauli spinors for spin and isospin. The wave function with proper boundary conditions for an emitted pion with asymptotic momentum $\vec{q}$ is $\phi^{(-)}_\pi(\vec{q}\,',\vec{q})$ and is distorted by the conjugate of the optical potential.[28] However, it is related to the pion wave function obtained from the optical potential itself, by $\phi^{(-)*}_\pi(\vec{q}\,',\vec{q})=\phi^{(+)}_\pi(\vec{q}\,',\vec{q})$.

A convenient form for evaluating the single particle matrix elements is the LS coupling scheme where the orbital angular momenta l and l' are coupled to L, the spins to S, and L and S are finally coupled to J the total single particle transition spin which, in a single particle model, is the transition spin of the nucleus. Inserting Eqs. (7) and (9) into Eq. (8) we obtain

$$\langle\alpha';\pi\,|\,t\,|\,\alpha;\gamma\rangle=\sum_{L,S,J,M}i^s(-1)^{j-m+(1/2)-m'_\tau+l'+S}\sqrt{6}\hat{j}\hat{j}'\hat{L}\hat{S}\hat{J}\begin{bmatrix}\frac{1}{2} & \frac{1}{2} & 1\\ -m'_\tau & m_\tau & -\beta\end{bmatrix}\begin{bmatrix}j' & j & J\\ -m' & m & M\end{bmatrix}\begin{Bmatrix}l' & \frac{1}{2} & j'\\ l & \frac{1}{2} & j\\ L & S & J\end{Bmatrix}I^{(a'a)LSJ}_{-M}\ , \tag{10}$$

where the integrals are,

$$I_M^{(a'a)LSJ}=\int d^3p\, d^3q'\rho_{a',a}(p',p)\phi_\pi^{(+)}(\vec{q}\,',\vec{q})[[Y^{l'}(\hat{p}\,')\times Y^l(\hat{p})]^L\times K^S]^J_M\ . \tag{11}$$

The momentum overlap distribution ρ is given in general by

$$\rho_{a',a}(p',p)=\phi^*_{n'l'j'}(p')\phi_{nlj}(p)\ , \tag{12}$$

where we have made no approximation other than assuming a one-body operator. If we restrict ourselves to the $1p$ shell and use harmonic oscillator wave functions with oscillator parameter b, the momentum distribution becomes

$$\rho(p'p)=\frac{8b^5}{3\sqrt{\pi}}pp'\exp\left[-\frac{b^2}{2}(p'^2+p^2)\right]\ , \tag{13}$$

which is independent of a' and a, and thus the integrals of Eq. (11) become independent of a' and a by replacing l' and l by 1.

While both the momentum distribution and the pion wave function are independent of the specific nuclear transition, the tensor operator determines the magnitude and importance of the various matrix elements. Compact analytic expressions for these operators are given in Ref. 29 for $J=0$ and 1. In general, we use the definition of the tensor product to obtain

$$[[Y^l(\hat{p}\,')\times Y^l(\hat{p})]^L\times K^S]^J_M=\frac{3}{4\pi pp'}\sum_{\substack{m_1,m_2\\M_L,M_S}}(1m_1 1m_2\,|\,11LM_L)(LM_LSM_S\,|\,LSJM)p'_{m_1}p_{m_2}K^S_{M_S}\ , \tag{14}$$

where p'_{m_1}, p_{m_2} are given in the spherical basis, e.g.,

$$p_m=\begin{cases}p\cos\theta_p & m=0\\ \mp 1/\sqrt{2}\,p\sin\theta_p(\cos\phi_p\pm i\sin\phi_p) & m=\pm 1\end{cases} \tag{15}$$

with θ_p the polar angle of $\vec{p}$ with respect to the incoming photon beam, and ϕ_p the azimuthal angle of $\vec{p}$ measured with respect to the pion production plane.

III. PION WAVE FUNCTION IN MOMENTUM SPACE

For calculating the integrals of Eq. (11) we need a distorted pion wave function in momentum space. Starting from a standard solution of an optical potential in coordinate space,[30] we perform a Fourier transformation into momentum space. Thus,

$$\phi_\pi^{(+)}(\vec{q}\,',\vec{q})=\frac{1}{(2\pi)^3}\int d^3r\, e^{-i\vec{q}\,'\cdot\vec{r}}\phi_\pi^{(+)}(\vec{r},\vec{q})\ , \tag{16}$$

where the plus sign denotes the boundary condition for outgoing waves. We can expand $\phi_\pi^{(+)}$ in partial waves by,

$$\phi_\pi^{(+)}(\vec{r},\vec{q})=4\pi\sum_{lm}i^l U_{l,q}(\hat{r})Y_l^m(r)Y_l^{m*}(q)\ , \tag{17}$$

where the asymptotic form of $U_{l,q}(r)$ is,

$$U_{l,q}(r)\sim\tfrac{1}{2}[e^{2i\delta_l}U_l^+(qr)+U_l^-(qr)]\ , \tag{18}$$

and δ_l is the nuclear plus Coulomb phase shift. The asymptotic expansion of the outgoing Coulomb function is

$$U_l^+(qr)=\frac{e^{i[qr-\eta\ln(2qr)-\pi(l+1)/2]}}{qr}\times{}_2F_0\left[l+1+i\eta,-l+i\eta;\frac{1}{2iqr}\right]\ , \tag{19}$$

where the Sommerfeld parameter $\eta=\alpha Z/v$, and $U_l^-=U_l^{+*}$. We turn off the Coulomb potential by taking $\eta\to 0$ and find,

$$\lim_{\eta\to 0}U_l^+(qr)=h_l^{(1)}(qr)\ . \tag{20}$$

Substituting Eq. (17) into Eq. (16), we obtain the following expression for the pion wave function in momentum space:

$$\phi_\pi^{(+)}(\vec{q}\,',\vec{q})=\frac{1}{2\pi^2}\sum_l(2l+1)P_l(\hat{q}\cdot\hat{q}\,')\times\int_0^\infty r^2 j_l(q'r)U_{l,q}(r)dr\ . \tag{21}$$

The integral in Eq. (21) cannot be evaluated numerically due to its behavior at infinity, so we separate it into two terms by writing

$$U_{l,q}(r)=U^{\rm int}_{l,q}(r)+U^{\rm asym}_{l,q}(r)\ ,$$

where

$$U^{\rm int}_{l,q}(r)=U_{l,q}(r)-U^{\rm asym}_{l,q}(r)\ . \tag{22}$$

The integral over $U^{\rm int}_{l,q}$ can be restricted to $r\le R$ where R is the order of a few nuclear radii, while the Fourier transform of the asymptotic wave function will be carried out analytically. Furthermore, to reduce the l sum in Eq. (21) we ad and subtract the term

$$\delta(\vec{q}-\vec{q}\,')=\sum_l(2l+1)/4\pi P_l(\hat{q}\cdot\hat{q}\,')\delta(q-q')/q^2\ .$$

Thus we must evaluate

$$\phi_\pi^{(+)}(\vec{q}\,',\vec{q})=\delta(\vec{q}-\vec{q}\,')+\frac{1}{2\pi^2}\sum_l(2l+1)P_l(\hat{q}\cdot\hat{q}')\left[\int_0^R j_l(q'r)U_{l,q}(r)r^2dr+I_l(q',q)-\frac{\pi}{2}\frac{\delta(q-q')}{q^2}\right], \tag{23}$$

where

$$I_l(q',q)=\int_0^\infty r^2 j_l(q'r)U_{l,q}^{\text{asym}}(r)dr\ . \tag{24}$$

For the simpler case without Coulomb ($\eta=0$), the asymptotic wave function $h_l^{(1)}(qr)=j_l(qr)+in_l(qr)$ involves only Bessel and Neumann functions for which we find the following Fourier transformations:

$$\int_0^\infty r^2 j_l(q'r)j_l(qr)dr=\frac{\pi}{2q^2}\delta(q'-q)\ , \tag{25}$$

$$\int_0^\infty r^2 j_l(q'r)n_l(qr)dr=\frac{q'^l}{q^{l+1}}\frac{\mathrm{P}}{q^2-q'^2}\ , \tag{26}$$

where P denotes a principal value integration. For this case,

$$I_l(q',q;\eta=0)=\frac{e^{2i\delta_l}+1}{4}\frac{\pi}{q^2}\delta(q-q')+\frac{e^{2i\delta_l}-1}{2}\frac{q'^l}{q^{l+1}}\frac{\mathrm{P}}{q^2-q'^2}\ . \tag{27}$$

Therefore the momentum space representation of the pion wave function is of functional form rather than a function as in coordinate space. Substituting the wave function into Eq. (11) we have to integrate over $\vec{q}\,'$, so I_l is properly defined. To avoid numerical difficulties we perform the principal value integral using the following prescription:

$$\mathrm{P}\int_0^{q'_{\max}}\frac{q'^{l+2}}{q^{l+1}}\frac{F(q')}{q^2-q'^2}dq'=\int_0^{q'_{\max}}dq'\frac{q'}{q^2-q'^2}\left[\frac{q'^{l+1}}{q^{l+1}}F(q')-F(q)\right]+\frac{F(q)}{2}\ln\frac{q^2}{q'^2_{\max}-q^2}\ . \tag{28}$$

For the $\eta=0$ case, these techniques allow for the Fourier transformation of the pion wave function and the subsequent integration over d^3q'. Note that the terms $I_l-\pi\delta(q'-q)/2q^2$ in Eq. (23) are all proportional to $(e^{2i\delta_l}-1)$ and therefore go to zero for nonpenetrating pion orbits.

For Coulomb waves, the Fourier transformation is more difficult. Firstly, we cannot use the full asymptotic solution given in Eq. (19) since the integrand diverges at the origin for the higher terms of ${}_2F_0$. However, the Fourier transformation of the first $l+2$ terms of U_l^+ is well defined. Consider

$$I_l^+=\int_0^\infty e^{-\epsilon r}j_l(q'r)U_l^+(qr)r^2dr\ , \tag{29}$$

where $\epsilon>0$ provides the convergence of the integral at infinity and

$$U_l^+(qr)=\frac{e^{i[qr-\eta\ln(2qr)-\pi(l+1)/2]}}{qr}\sum_{m=0}^{l+2}\frac{(l+1+i\eta)_m(-l+i\eta)_m}{m!(2iqr)^m}\ . \tag{30}$$

Since j_l is real, $I_l^-=I_l^{+*}$. Writing $j_l=(h_l^{(1)}+h_l^{(2)})/2$, and using the finite term expansion for the spherical Hankel function, we can integrate Eq. (29) term by term to obtain

$$I_l^+=\frac{e^{-i[\eta\ln(2q)-(l+1)\pi]}}{2qq'}\Gamma(1-i\eta)\sum_{m=0}^{l+2}\sum_{n=0}^{l}\frac{(l+1+i\eta)_m(-l+i\eta)_m}{(i\eta)_{m+n}(-2iq)^m(-2iq')^n}\times\frac{(l+1)_n(-l)_n}{m!n!}[\Delta_+^{m+n-1+i\eta}+(-1)^{l+n+1}\Delta_-^{m+n-1+i\eta}]\ , \tag{31}$$

where $\Delta_+=\epsilon-i(q+q')$ and $\Delta_-=\epsilon-i(q-q')$.

As in the $\eta=0$ case, the quantity I_l^+ is singular when $q'\to q$, but the quantity

$$E_l^+=\lim_{\substack{q'\to q\\ \epsilon\to 0}}(\Delta_+\Delta_-)^{1-i\eta}I_l^+=\frac{2i(-1)^l e^{-\eta\pi/2}}{(2q)^{1+2i\eta}}\Gamma(1-i\eta) \tag{32}$$

is well defined. Thus, we write

$$\int_0^{q'_{\max}}F(q')I_l^+(q')q'^2dq'=\lim_{\epsilon\to 0}\int_0^{q'_{\max}}\frac{q'dq'}{(\Delta_+\Delta_-)^{1-i\eta}}[q'(\Delta_+\Delta_-)^{1-i\eta}I_l^+(q')F(q')-qF(q)E_l^+(q)]+\frac{qF(q)E_l^+(q)}{2i\eta}[(q'^2_{\max}-q^2)^{i\eta}-q^{2i\eta}e^{\eta\pi}]\ . \tag{33}$$

The equivalent results for I_l^- follow by complex conjugation for all but $F(q')$.

Even though formally correct, a numerical application still is nontrivial. So far we have not included the Coulomb

wave function into our calculations and all nonlocal results shown further on are obtained with the Coulomb potential neglected. Since our calculations are performed at pion energies of 50 MeV and more this approximation is of minor importance.

IV. PWIA AND LOCAL APPROXIMATION

At this point it is useful to discuss some approximations and simplifications of Eq. (11) that are commonly made. Firstly, we derive the PWIA by replacing the pion wave function with a delta function, which is the free pion solution

$$\phi_\pi^{(+)}(\vec{q}\,',\vec{q})=\delta(\vec{q}\,'-\vec{q}) \tag{34}$$

which leads to the nonlocal PWIA result

$$I_M^{(a'a)LSJ}=\int d^3p\,\rho_{a'a}(p',p)[[Y^{l'}(\hat{p}')\times Y^{l}(\hat{p})]^L\times K^S]^J_M\ . \tag{35}$$

Furthermore, if the operator K^S is local in that it does not depend on the initial nucleon momentum $\vec{p}$, a Fourier transformation into r space is possible and leads to the numerically simpler expression for the local PWIA

$$I_M^{(a'a)LSJ}=(-i)^L\sqrt{4\pi}\hat{l}'\hat{l}\begin{bmatrix} l' & l & L \\ 0 & 0 & 0 \end{bmatrix}[Y^L(\hat{Q})\times K^S]^J_M\int dr\,r^2\rho_{a'a}(r)j_L(Qr)\ , \tag{36}$$

where $\vec{Q}=\vec{k}-\vec{q}$ is the momentum transfer to the nucleus and $\rho_{a'a}$ is the transition density which for the harmonic oscillator $1p$ shell is given by

$$\rho(r)=\frac{8}{3b^5\sqrt{\pi}}r^2\exp(-r^2/b^2)\ . \tag{37}$$

Finally we can use a partial wave expansion of the pion wave [see Eq. (17)] as well as the photon to obtain the local DWIA result,

$$I_M^{(a'a)LSJ}=4\pi\sum_{l_\gamma,l_\pi}(i)^{l_\gamma+l_\pi}(-1)^{l_\pi+L}\hat{l}_\gamma\hat{l}_\pi\hat{l}'\hat{l}\begin{bmatrix} l_\gamma & l_\pi & L \\ 0 & 0 & 0 \end{bmatrix}\begin{bmatrix} l' & l & L \\ 0 & 0 & 0 \end{bmatrix}[[Y^{l_\gamma}(\hat{k})\times Y^{l_\pi}(\hat{q})]^L\times K^S]^J_M\int dr\,r^2\rho_{a'a}(r)U_{l_{\pi,q}}(r)j_{l_\gamma}(kr)\ . \tag{38}$$

The tensor operators appearing in this expression are most simply evaluated by

$$[[Y^{l_\gamma}(\hat{k})\times Y^{l_\pi}(\hat{q})]^L\times K^S]^J_M=\frac{1}{4\pi}\hat{l}_\gamma\hat{l}_\pi\hat{L}\hat{J}\sum_{M_S}(-1)^{S-M_S}\left[\frac{(l_\pi-m_\pi)!}{(l_\pi+m_\pi)!}\right]^{1/2}\times\begin{bmatrix} L & S & J \\ m_\pi & M_S & -M \end{bmatrix}\begin{bmatrix} l_\pi & l_\gamma & L \\ m_\pi & 0 & -m_\pi \end{bmatrix}P_{l_\pi}^{m_\pi}(\cos\theta_\pi)K^S_{M_S}\ , \tag{39}$$

where $P_{l_\pi}^{m_\pi}$ is the associated Legendre function of degree l_π and order $m_\pi=M-M_S$.

The four formulae of Eqs. (11), (35), (36), and (38) give only the extreme ways of treating nonlocalities. In Eqs. (11) and (35) they are treated exactly, while in Eqs. (36) and (38) nonlocalities are ignored completely. In other theoretical work[2,17] nonlocalities have been partially included by replacing $\vec{p}\rightarrow -i\vec{\nabla}$, acting on the single particle wave function, and $\vec{q}\rightarrow -i\vec{\nabla}$, acting on the pion wave function. These calculations, however, ignore the energy and momentum dependence of the propagators and presumably their validity is somewhat between our local and our nonlocal distorted wave calculations. Recently Toker and Tabakin[22] have investigated propagator nonlocalities and found them to be very important, especially in pion photoproduction from ^{14}N where the local Kroll-Ruderman term ($\vec{\sigma}\cdot\vec{\epsilon}$) is suppressed. As noted in the Introduction, they include nonlocalities in a mixed coordinate momentum space calculation. Our method of handling nonlocalities by working in momentum space is more straightforward, but does require extensive numerical integration to evaluate Eq. (11). However, any operator based on diagrammatic techniques, nonrelativistic or relativistic, can be used; and any pion wave function, apart from Coulomb effects as of now, can easily be obtained as a Fourier transform of the coordinate space solution. Alternatively, direct use of existent momentum space solutions for optical potentials could be easily included in our framework.

V. PARTIAL CROSS SECTIONS

Putting our results together, we insert the nuclear matrix elements of Eq. (6) and the single particle matrix elements of Eq. (10) into Eq. (4) and carry out the spin projection summations to obtain,

$$\sum_{M_i,M_f,\lambda} |\langle J_f M_f, T_f N_f;\pi | T | J_i M_i, T_i N_i;\gamma\rangle|^2 = \sum_{J,M,\lambda} |F_M^J|^2 , \tag{40}$$

where

$$F_M^J = \begin{bmatrix} T_f & 1 & T_i \\ -N_f & -\beta & N_i \end{bmatrix} \sqrt{6} \sum_{a'a} \psi_{J;1}(a',a) \sum_{LS} (-i)^S (-1)^{l'+1} \hat{j}' \hat{j} \hat{L} \hat{S} \begin{Bmatrix} l' & \frac{1}{2} & j' \\ l & \frac{1}{2} & j \\ L & S & J \end{Bmatrix} I_M^{(a',a)LSJ} . \tag{41}$$

As discussed above, by using harmonic oscillator orbitals the integrals I_M^{LSJ} become independent of a',a and we can perform the summation over the single particle states $a,a' = 1p_{3/2}, 1p_{1/2}$ to obtain

$$F_M^J = \begin{bmatrix} T_f & 1 & T_i \\ -N_f & -\beta & N_i \end{bmatrix} \sqrt{6} \sum_{LS} (-i)^S \psi_{J(LS);1} I_M^{LSJ} , \tag{42}$$

where $\psi_{J(LS);T}$ is the reduced density matrix element of a specific nuclear transition in the LS-coupling scheme. This representation has the great advantage that each $\psi_{J(LS)}$ corresponds to one pion production integral I^{LSJ} which has a specific dependence on spin and angular momentum transfer. Later in this paper we will see that these integrals show quite different behavior with respect to nonlocalities, pion distortions, and the delta isobar term in the production operator. To discuss these effects in a more general way we introduce a new way of writing the differential cross section by combining Eqs. (1) and (42) to write

$$\frac{d\sigma}{d\Omega_\pi^{\text{c.m.}}} = 6 \frac{\begin{bmatrix} T_f & 1 & T_i \\ -N_f & -\beta & N_i \end{bmatrix}^2}{2J_i+1} \sum_{\substack{\alpha,\alpha' \\ \alpha' \le \alpha}} \psi_{\alpha'} \psi_\alpha \sigma_{\alpha'\alpha} \tag{43}$$

with $\alpha = \{(LS)J;T=1\}$ as illustrated in Table I. The "partial" cross sections $\sigma_{\alpha'\alpha}$ no longer depend very strongly on nuclear structure and are given by

$$\sigma_{\alpha'\alpha} = \frac{\alpha}{8\pi} \frac{q^{\text{c.m.}}}{k^{\text{c.m.}}} \frac{m_i m_f}{W^2} \mathcal{F}_{\text{c.m.}} \sum_{M,\lambda} \text{Re}\{(-i)^{S'-S} I_M^{\alpha'*} I_M^\alpha\} \times (2-\delta_{\alpha'\alpha}) \delta_{J'J} . \tag{44}$$

TABLE I. Reduced density matrix elements $\psi_\alpha \equiv \psi_{J(LS);T=1}$ in LS coupling. Matrix elements which also contribute in a local approximation are marked by an asterisk.

α	J	L	S
1	0	0	0*
2	0	1	1
3	1	1	0
4	1	0	1*
5	1	1	1
6	1	2	1*
7	2	2	0*
8	2	1	1
9	2	2	1*
10	3	2	1*

Thus apart from small nuclear structure effects which are hidden in the integrals I_M^α in the form of the oscillator parameter b and the pion wave function, the partial cross sections are the same for all pion photoproduction reactions in the $1p$ shell from ^{6}Li to ^{15}N.

The partial cross sections can be displayed in the form of a 10×10 matrix,

$$\{\sigma_{\alpha'\alpha}\} = \begin{bmatrix} J=0 & 0 & 0 & 0 \\ 0 & J=1 & 0 & 0 \\ 0 & 0 & J=2 & 0 \\ 0 & 0 & 0 & J=3 \end{bmatrix} , \tag{45}$$

where each transition spin J represents a matrix itself since there is no interference between different J values. For $J=0$, 1, 2, and 3 the submatrices are of dimensions 2, 4, 3, and 1, respectively,

$$\text{for } J=0: \begin{bmatrix} \underline{\sigma}_{11} & \sigma_{12} \\ 0 & \sigma_{22} \end{bmatrix} ,$$

$$\text{for } J=1: \begin{bmatrix} \sigma_{33} & \sigma_{34} & \sigma_{35} & \sigma_{36} \\ 0 & \underline{\sigma}_{44} & \sigma_{45} & \underline{\sigma}_{46} \\ 0 & 0 & \sigma_{55} & \sigma_{56} \\ 0 & 0 & 0 & \underline{\sigma}_{66} \end{bmatrix} , \tag{46}$$

$$\text{for } J=2: \begin{bmatrix} \underline{\sigma}_{77} & \sigma_{78} & \underline{\sigma}_{79} \\ 0 & \sigma_{88} & \sigma_{89} \\ 0 & 0 & \underline{\sigma}_{99} \end{bmatrix} ,$$

$$\text{for } J=3: \underline{\sigma}_{10,10} ,$$

where only the underlined elements are nonzero in a local calculation. From the parity three-j symbol

$$\begin{bmatrix} l' & l & L \\ 0 & 0 & 0 \end{bmatrix}$$

in Eqs. (36) and (38) we can see that for the $1p$ shell with $l'=l=1$ only $L=0$ and 2 contribute. Therefore all terms $\sigma_{\alpha'\alpha}$ with α' or α equal to 2, 3, 5, or 8 vanish in the local approximation according to Table I.

VI. MODEL INGREDIENTS

One of the basic ingredients of a DWIA calculation is the elementary pion photoproduction operator of Eq. (4). Three developments are in wide use, the Berends,[31] the Chew, Goldberger, Low, and Nambu (CGLN),[32] and the Blomqvist-Laget[33] amplitudes. All give a satisfactory

description of pion photoproduction from the nucleon. However, only the amplitude of Blomqvist and Laget is suitable for using in a nonlocal calculation on nuclei. The Blomqvist-Laget operator is a nonrelativistic reduction of covariant Feynman amplitudes and can be evaluated in an arbitrary reference frame. Furthermore, by treating energy and momentum components as independent variables a straightforward off-shell extrapolation can be defined which allows the study of off-shell effects in nuclei. In the Appendix we give the formulae for the spin decomposed amplitudes L and $\vec{K}$ of Eq. (4) for both π^+ and π^- with the pseudovector Born terms and the $\Delta(1236)$ excitation term written out separately. The differential cross section for both $\gamma + p \rightarrow \pi^+ + n$ and $\gamma + n \rightarrow \pi^- + p$ in this notation is given by

$$\frac{d\sigma}{d\Omega_\pi^{\text{c.m.}}} = \frac{\alpha}{8\pi} \frac{q^{\text{c.m.}}}{k^{\text{c.m.}}} \frac{m^2}{W^2} \sum_\lambda (|L|^2 + |\vec{K}|^2) , \quad (47)$$

which shows the well-known fact that in the nucleon case the spin transitions $S=J=0$ and $S=J=1$ contribute equally to the cross sections. This is not the case for pion production in nuclei, where the values of the nuclear matrix elements determine this ratio. For example, in the reaction $^{13}C(\gamma,\pi^-)^{13}N_{g.s.}$ the matrix elements favor $S=0$, whereas in the $^{12}C(\gamma,\pi^+)^{12}B_{g.s.}$ the $S=1$ transitions dominate. Therefore a good fit of differential and total cross sections for the elementary process does not necessarily provide the same quality of fit for all nuclear physics reactions.

The second major ingredient of a DWIA calculation is the pion optical potential. This has been studied most extensively by the group of Stricker, McManus, and Carr.[34–36] Their analyses provide good fits to low energy pion scattering on light nuclei.[35,36] For higher energies up to $T_\pi = 220$ MeV they give an extrapolation of the optical potential parameters which also gives satisfactory agreement with experimental data.[34] We have followed the method of Ref. 2 and obtain an energy dependent optical potential from threshold up to 220 MeV by linearly interpolating the parameters. This gives smooth energy-dependent pion wave functions which cover the whole kinematical range of our calculations, from pion production threshold up to photon energies of 400 MeV.

VII. RESULTS

To check our nonlocal code, the number of integration points in the six-dimensional integral in Eq. (11) was varied over a wide range. For the energies considered in this paper, about 300 000 integration points gave results good to 2%. We checked the code further by inserting numerically a plane wave pion wave function into Eq. (11) and comparing the result to that obtained using Eq. (35). In addition, we put a local K^s operator into Eq. (11) and compared the result to the simple result given in Eq. (36). We always obtained excellent agreement.

Rather than examining a large number of specific pion production reactions which depend strongly on particular nuclear matrix elements, we want to study nonlocal effects and pion distortion effects on the partial cross sections defined in Eq. (44). As we mentioned previously, the partial cross sections depend on nuclear structure only through the oscillator range parameter b, which varies in the $1p$ shell from 1.57 to 2.03 fm, and slight changes of the pion optical model wave functions from one nucleus to another. For carrying out our study we chose the reaction $^{13}C(\gamma,\pi^-)^{13}N_{g.s.}$, but calculated all partial cross sections for $E0$, $M1$, $E2$, and $M3$ multipoles, although $E2$

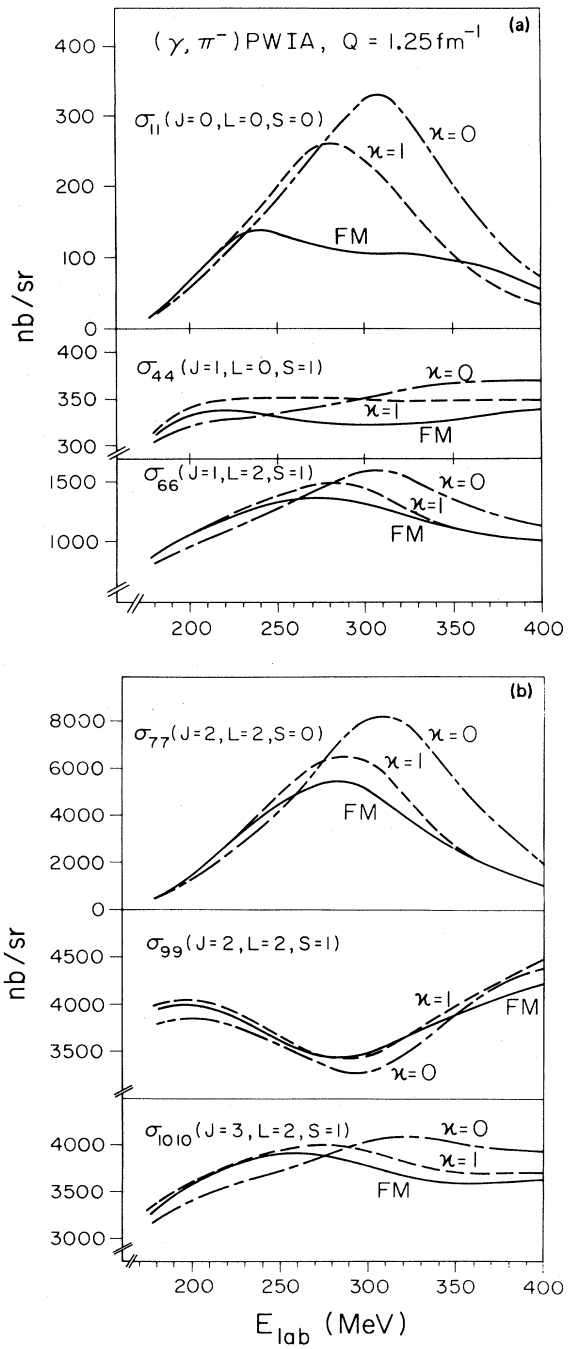

FIG. 3. Partial cross sections $\sigma_{\alpha\alpha}$ for γ,π^- on p-shell nuclei at $Q=1.25$ fm^{-1} as a function of photon energy. The full, dashed, and dash-dotted lines are PWIA calculations with exact Fermi motion (FM), local on-shell approximation ($\kappa=1$), and frozen nucleon approximation ($\kappa=0$), respectively.

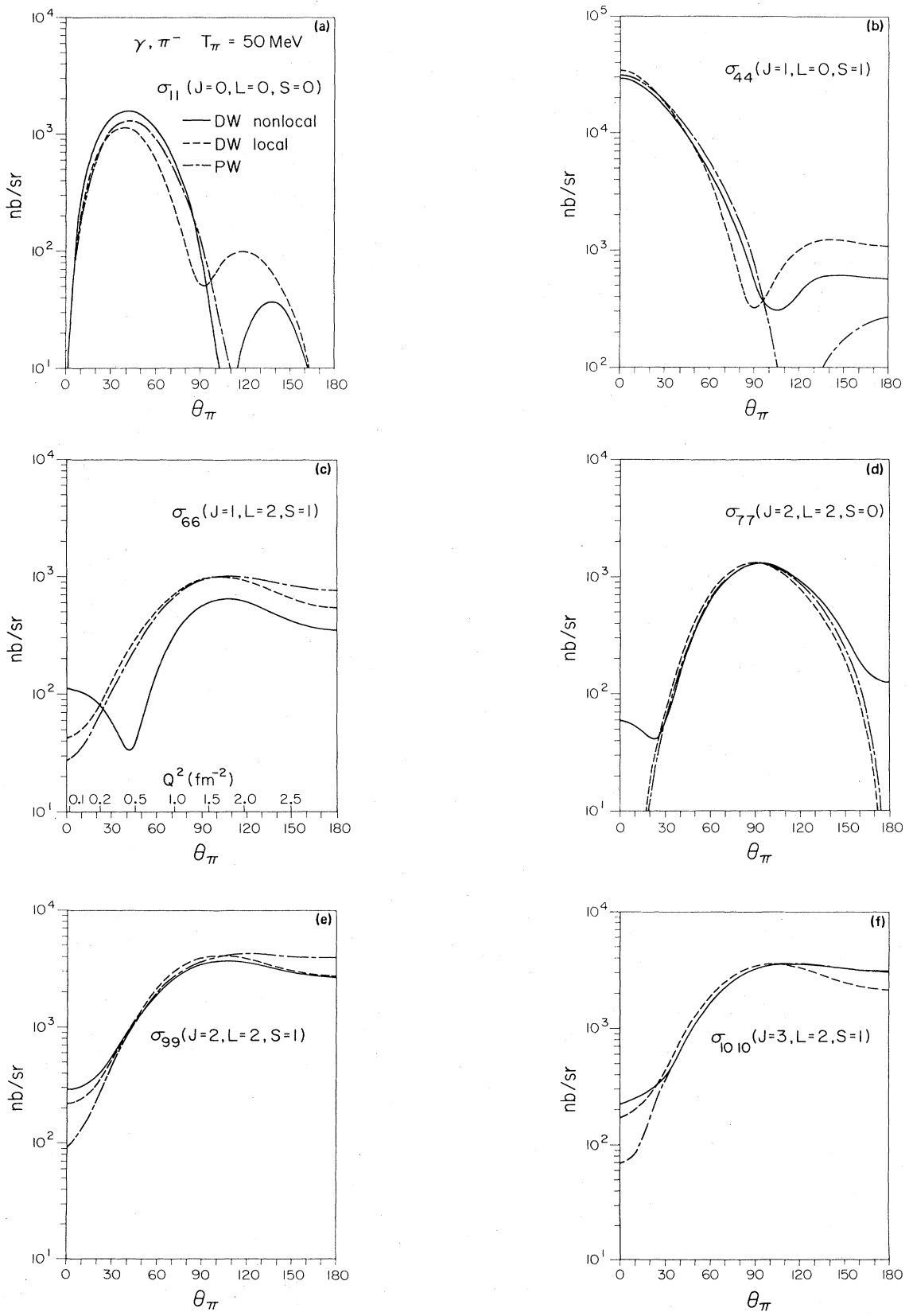

FIG. 4. Angular distributions of partial cross sections $\sigma_{\alpha\alpha}$ for γ,π^- at $T_\pi=50$ MeV. The full and dashed curves are nonlocal and local ($\kappa=1$) DWIA calculations, the dash-dotted lines are PWIA calculations with Fermi motion. All cross sections are given in nb/sr.

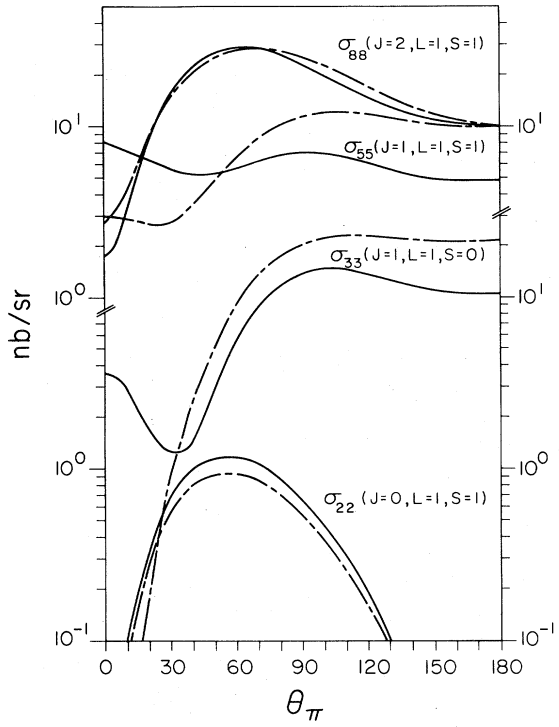

FIG. 5. The same as Fig. 4 for the purely nonlocal partial cross sections σ_{22}, σ_{33}, σ_{55}, and σ_{88}, all with $L=1$.

and $M3$ do not contribute for this specific transition. We chose the harmonic oscillator parameter $b=1.73$ fm.

First we consider the plane wave approximation [Eq. (35)]. In this case nonlocal effects arise entirely from nucleon Fermi motion. For light nuclei such as ^{3}He, the effects of Fermi motion have been studied earlier, and were found to contribute mainly in the Δ resonance region.[29] Near threshold, Fermi motion contributed less than 5% (Ref. 37). We find a similar result for p-shell nuclei. At energies below the Δ resonance the Fermi motion effects are very small and at a typical pion energy of 50 MeV they can be neglected. In the resonance region, the partial cross sections show some interesting effects. In Fig. 3 we show the six dominant diagonal elements of $\sigma_{\alpha'\alpha}$ for a constant momentum transfer $Q=1.25$ fm^{-1} as a function of the photon energy. The label κ in the figure defines the average momentum of our local approximation

$$\langle \vec{p} \rangle = -\kappa \frac{A-1}{2A} \vec{Q} ,$$

where $\kappa=0$ is a frozen nucleon approximation, and $\kappa=1$ is an on-shell approximation which worked rather well for ^{3}He$(\gamma,\pi^+)^3$H (Ref. 29). We find a similar result here. In all cases, the $\kappa=1$ agrees better with the exact treatment of Fermi motion than $\kappa=0$. For the partial cross section σ_{11} ($E0$) the effects are the largest, with neither approximation reproducing the large broadening and the shift of the resonance resulting from Fermi motion. The $M1$ terms, σ_{44} and σ_{66}, are not very sensitive to Fermi motion and neither is the $M3$ term $\sigma_{10,10}$. In the $E2$ terms, we get only a small effect in σ_{99}, while σ_{77} shows effects similar

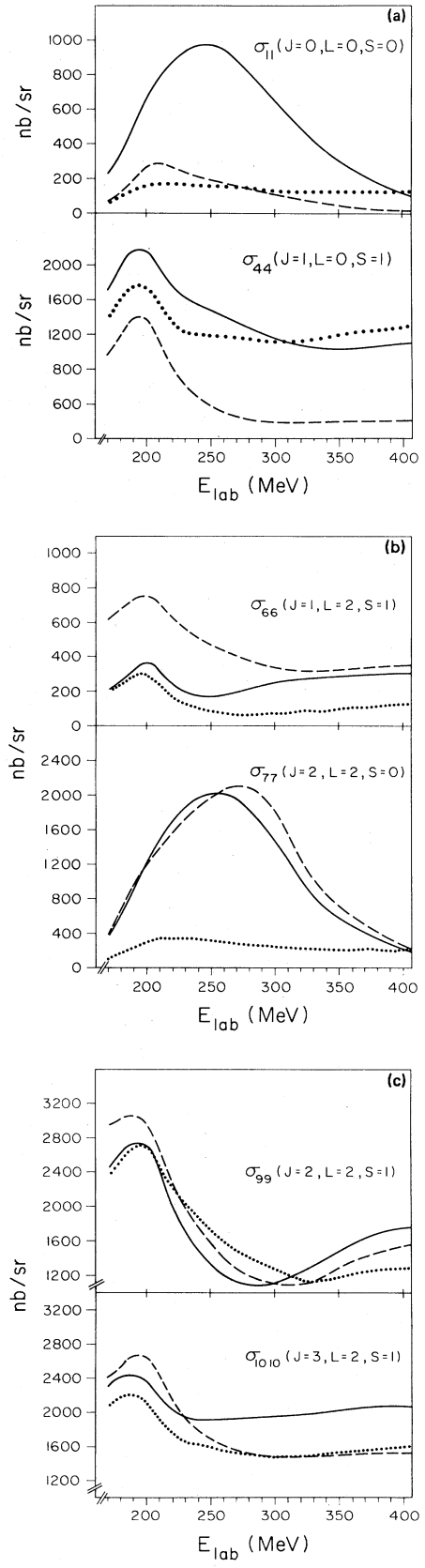

FIG. 6. Partial cross sections $\sigma_{\alpha\alpha}$ in the Δ region at $Q=1.0$ fm^{-1}. The dotted lines are nonlocal DWIA calculations with Δ excitation omitted. Everything else as in Fig. 4.

to those in σ_{11}. These results have a simple explanation since both $\alpha=1$ and 7 are $S=0$ transitions which are proportional to the L part of the elementary amplitude which is dominated by the Δ resonance. All other transitions are proportional to $\vec{K}$, and therefore are dominated by the Kroll-Ruderman term.

In Fig. 4 we show the effect of pion distortion on the partial cross sections at low energy. Except for minima, the local DWIA calculations [Eq. (38)] are close to the PWIA results, but the full DWIA [Eq. (11)] calculations show substantial changes; for $E0$ transitions in the minima and for $M1$ transitions for angles larger than 90°. These nonlocal effects are totally different from Fermi motion effects; they arise from the smearing of the pion momentum by the optical potential. And except for energies very close to threshold, the pion momentum dependence of the elementary operator is always important.

The role played by the purely nonlocal terms $\sigma_{\alpha\alpha}$ with $\alpha=2$, 3, 5, and 8, shown in Fig. 5, is not very important as long as there is no cancellation of the other larger contributions due to nuclear structure. In general, they are smaller than other terms by at least one order of magnitude, so their role is limited. The influence of pion distortions on these terms is similar to those in Fig. 4.

When the energy of the photon increases and reaches the Δ resonance region the nonlocal effects from both nucleon Fermi motion and pion momentum smearing work together. In Fig. 6 the six major contributions are shown at a constant momentum transfer $Q=1.0$ fm^{-1} as functions of the photon energy. Here very large nonlocal effects arise in the $E0$ cross section σ_{11} where a big bump with a peak around 240 MeV shows up in the nonlocal calculation. Further nonlocal effects are very important in both $M1$ cross sections as well as to some extent in $M3$ at high energies, whereas the $E2$ contributions are less sensitive to nonlocalities. A plane wave impulse approximation is not compared in this figure but is qualitatively the same as in Fig. 3. While the shape is similar to the $S=0$ transitions (σ_{11} and σ_{77}) but far too big in comparison with the distorted calculations, in all other reduced cross sections both shape and magnitude of plane wave and distorted wave calculations are very different for energies above 250 MeV. In all $S=1$ transitions a small peak around 200 MeV arises from the optical potential and has nothing to do with the Δ resonance. This can easily be seen by removing the Δ excitation part from the Blomqvist-Laget operator as demonstrated in Fig. 6.

VIII. APPLICATION TO ^{13}C

While low energy pion production on light nuclei like ^{6}Li, ^{10}B, and ^{12}C has been described reasonably well by theory,[2] two experiments on ^{13}C at $\theta_\pi=90°$ and $T_\pi^{\rm lab}=18$, 30, and 42 MeV have shown a large discrepancy between theory and experiment.[11,12] Using Cohen-Kurath matrix elements and harmonic oscillator wave functions the theoretical distorted wave calculations overestimated the data by factors up to 20 (Ref. 11). For $^{13}C(\gamma,\pi^+)^{13}B_{g.s.}$, Cheon[38] found a reasonable description of the data by defining effective charges for the p-shell protons and Sata, Koshigin, and Ohtsubo (see Ref. 39) obtain a similar result by using radial wave functions with core-polarization corrections. In both analyses the crucial point is that the nuclear wave functions are changed to achieve better agreement with the 15.11 MeV transverse form factor in ^{13}C, the analog state of $^{13}B_{g.s.}$ (see Fig. 7). In $^{13}C(\gamma,\pi^-)^{13}N_{g.s.}$ the harmonic oscillator model and Cohen-Kurath wave functions again overestimate the elastic $M1$ form factor, but in a somewhat different approach, constraining the reduced density matrix elements to fit experimental information on form factor, magnetic moments, and β decay could explain most of the discrepancies between theory and experiment.[20] In addition to nuclear structure effects which are very important in ^{13}C, we can expect large nonlocal effects. Because $J_i=J_f=\frac{1}{2}$ there are $E0$ and $M1$ transitions possible and both show sensitivity to nonlocalities even at low energies (see Fig. 4). In Fig. 8 we show, in an angular distribution for $^{13}C(\gamma,\pi^-)^{13}N_{g.s.}$, the differences between local and nonlocal distorted wave calculations and compare them with preliminary data of Stoler *et al.*[23] While the $E0$

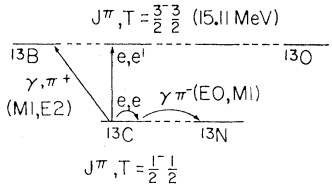

FIG. 7. Isobar diagram for $A=13$. Only the levels involved in the reactions $^{13}C(\gamma,\pi^-)^{13}N_{g.s.}$ and $^{13}C(\gamma,\pi^+)^{13}B_{g.s.}$ are shown.

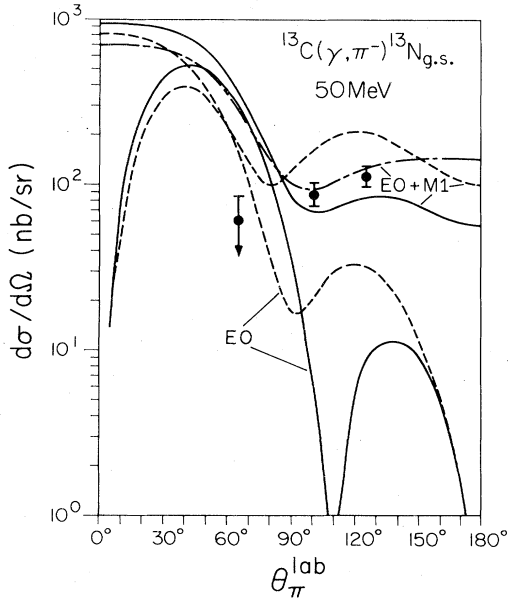

FIG. 8. Differential cross section in nb/sr for $^{13}C(\gamma,\pi^-)^{13}N_{g.s.}$ at $T_\pi=50$ MeV. $E0$ and $E0+M1$ contributions are given separately, see Fig. 4 for the meaning of the lines. The preliminary data points are from Stoler *et al.* (Ref. 23).

TABLE II. Reduced density matrix elements for the $^{13}C_{g.s.}$ wave function. The numbers are given both in jj coupling, $\psi_{J;T(j'j)}$ and LS coupling, $\psi_{J(LS);T}$.

		$(j'j)$				(LS)				
J	T	$\frac{1}{2}\frac{1}{2}$	$\frac{1}{2}\frac{3}{2}$	$\frac{3}{2}\frac{1}{2}$	$\frac{3}{2}\frac{3}{2}$	0 0	0 1	1 0	1 1	2 1
0	0	1.612			5.224	5.196			−1.700	
0	1	0.652			0.246	0.577			0.390	
1	0	−0.176	−0.406	+0.406	0.372		−0.182	0.465	0	−0.5
1	1	0.413	−0.044	+0.044	−0.051		−0.158	0.186	0	0.343

contribution is strongly dominated by σ_{11}, the $M1$ contribution comes from a coherent sum of $\alpha=3$, 4, and 6 transitions although the purely nonlocal $\alpha=3$ does not play an important role. The net effects of the nonlocalities in this specific case is an increase of the cross section at forward angles and a larger decrease (up to a factor of 2.5) at backward angles. The nuclear wave function used is given in Table II for both jj- and LS-coupling schemes. While $\psi_{0(00)}$, $\psi_{1(10)}$, $\psi_{1(01)}$, and $\psi_{1(21)}$ are taken from set II in Ref. 20, the missing $\psi_{0(11)}$, which cannot be determined from electron scattering at all, is taken from the shell model calculation of Ref. 40. However, the influence on γ,π at this low energy turns out to be very small, less than 4% of the $E0$ contribution. Finally, $\psi_{1(11)}\equiv 0$ because of time-reversal symmetry. While the data points at backward angles of 100° and 125° are in good agreement with our nonlocal calculations, the experiment at 65° shows an interesting suppression of the cross section which neither our plane wave, local nor nonlocal calculations can explain. However, since it appears in a region where the $E0$ contribution dominates, a plausible explanation could be an overestimate of $E0$ in our model. We will discuss this point further in Sec. IX.

A very interesting experiment could be performed in the minimum of the $M1$ form factor which would expose the $E0$ contribution of the cross section. While the minimum of the $M1$ form factor measured in elastic electron scattering[41] on ^{13}C appears at $Q=1.04$ fm^{-1}, in γ,π it will appear at a different momentum transfer in general. The reason is that in electron scattering both isoscalar and isovector transitions are allowed, and furthermore, the convection current contributes. In a PWIA pion production calculation this momentum shift can easily be calculated. The $M1$ form factor takes the general form[25]

$$F_{M1}\propto e^{-y}(A+By)$$

with $y=b^2Q^2/4$. Therefore the minimum shows up at $y_{\min}=-A/B$, which we can most simply express in terms of the LS-coupled nuclear density matrix elements. For the minimum of the isovector spin-flip form factor we find

$$y_{\min}=-\tfrac{3}{2}\sqrt{5}\psi_{1(01);1}/(\psi_{1(21);1}-\sqrt{5}\psi_{1(01);1})\,,$$

which takes the value of $y_{\min}=0.761$ fm^{-2} or $Q_{\min}=1.01$ fm^{-1} using the numbers from Table II. This value is very close to the minimum measured in (e,e'); however, this is purely accidental, and in $^{15}N(\gamma,\pi^-)^{15}O_{g.s.}$ the shift is quite large. Figure 9 shows our calculations at $Q=1$ fm^{-1}. The $E0$ contribution is clearly exposed in the nonlocal calculation, and the cross section follows the σ_{11} partial cross section from Fig. 6. Such an experiment would shed light on the production mechanism of pions in nuclei more than any experiment performed so far.

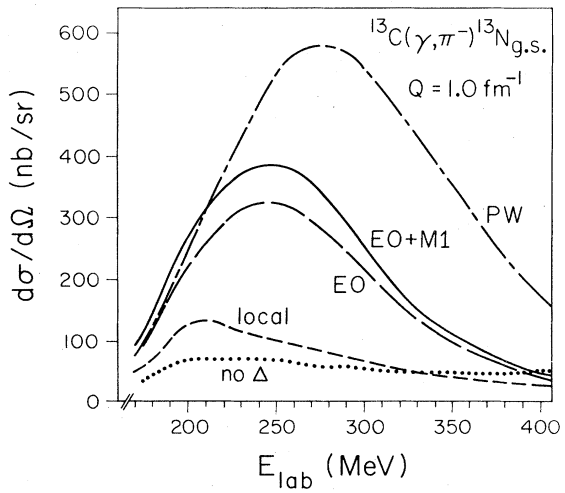

FIG. 9. Differential cross sections in nb/sr for $^{13}C(\gamma,\pi^-)^{13}N_{g.s.}$ at $Q=1.0$ fm^{-1} as function of photon energy. The full, short dashed, and dash-dotted lines are as in Fig. 4, the long dashed curve shows the $E0$ contribution alone, and the dotted line is $E0+M1$ with Δ omitted, both calculated in nonlocal DWIA.

IX. Δ-RESONANCE EFFECTS

From the derivation of elementary amplitudes for pion photoproduction it is well known that the Δ resonance plays an important role in the region around $E_\gamma=300$

TABLE III. Total cross sections in μb for pion photoproduction on the nucleon at $E_\gamma=310$ MeV ($W=1210$ MeV). Numbers are given separately for transition spin $S=0$ and 1. The separate contributions for pseudovector Born diagrams (PV) and Δ(1236) excitation add in a coherent way to the total result PV + Δ.

	$L(S=0)$			$K(S=1)$		
	PV	Δ	PV + Δ	PV	Δ	PV + Δ
$p(\gamma,\pi^+)n$	16	61	103	106	30	154
$n(\gamma,\pi^-)p$	16	61	102	161	30	216
$p(\gamma,\pi^0)p$	3	173	173	27	79	119
$n(\gamma,\pi^0)n$	3	173	173	13	79	101

MeV. In Fig. 10 we show the total cross section for π^- production on the neutron obtained with the model of Blomqvist and Laget.[33] However, here we have included the separate contribution for the $S=0$ and 1 transitions and point out the effect of the Δ resonance. While the role of the Δ is relatively unimportant for $S=1$ transitions (K) it plays a major role in the $S=0$ transitions (L). The situation for all possible $\gamma\pi$ reactions on the nucleons is shown in Table III. For neutral pion production the Δ dominates the cross section and it is a perfect doorway state for coherent π^0 production on nuclei, where only $S=0$ contributes. This is different for charged pion production, and for γ,π^- the Δ contributes 60% in $S=0$ and only 14% in $S=1$ transitions. Therefore in nuclear applications the Δ will never show up significantly in $M1$ and $M3$ transitions, since these are dominated by $S=1$. On the other hand it should be very important in $E0$ transitions and also in some $E2$ transitions. The best way to study this is an experiment which fixes the momentum transfer Q to the nucleus thereby keeping the nuclear transition form factor more or less constant. Then the role of the Δ can be examined by going from 200 to 400 MeV in photon energy. To demonstrate this, in Fig. 6 we have included the curves for the situation if no Δ were excited. As expected, the effects of the Δ are very big for the $S=0$ transitions (σ_{11} and σ_{77}) and are quite small for $S=1$. While the excitation of the Δ enhances the σ_{11} and σ_{77} by a factor of 6 in the maximum, the changes in the spin transitions is of the order of 30% and leads to both positive and negative interference with the Born terms. The biggest Δ effect in the spin transition is in σ_{66}, which normally plays a minor role in $M1$ transitions, which are dominated by the Gamow-Teller transition σ_{44}. However, in the 2.31 MeV transition of the $A=14$ system it will show up because of the suppression of the Gamow-Teller transition.

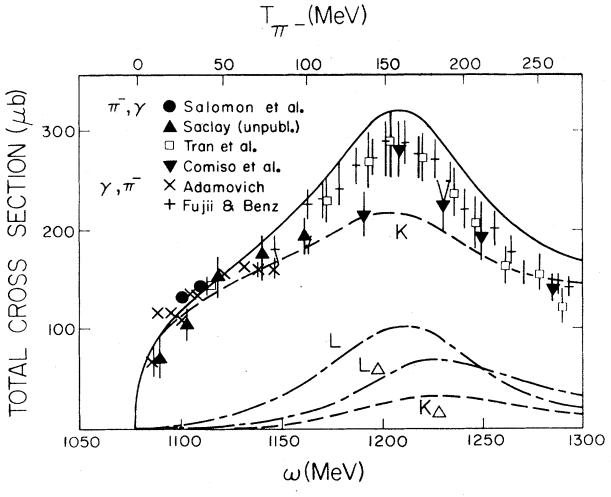

FIG. 10. Total cross section in μb for $\gamma n \to \pi^- p$. The full line shows the PV-Born + $\Delta(1236)$ model of Blomqvist-Laget, the dash-dotted lines (L,L_Δ) give the nonspin transitions ($S=0$), and the dashed lines (K,K_Δ) give the spin transitions ($S=1$), both for PV-Born + Δ and Δ separately. The data points are from Ref. 42 or quoted therein. Copied with permission.

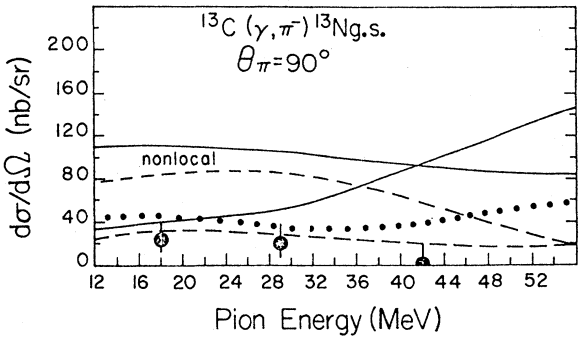

FIG. 11. Differential cross section in nb/sr for $^{13}C(\gamma,\pi^-)^{13}N_{g.s.}$ at $\theta_\pi=90°$ as a function of the pion laboratory energy. The full lines show $E0+M1$, the dashed lines $E0$ separately, both for nonlocal and local DWIA. The dotted line is obtained for nonlocal DWIA, $E0+M1$, where the Δ excitation is omitted. The data points are from LeRose *et al.* (Ref. 11).

The effect of the Δ on the specific reaction $^{13}C(\gamma,\pi^-)^{13}N_{g.s.}$ is demonstrated in Figs. 11 and 12. Because of the importance of the $E0$ contribution, even at low energies the effects are sizable. Figure 11 shows the old Bates experiment[11] at $\theta_\pi=90°$ which was in big disagreement with theory for some time. The consistent treatment of all nonlocalities of the full Blomqvist-Laget

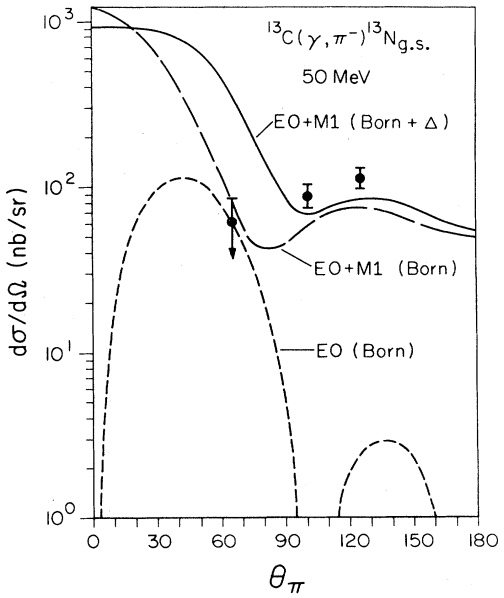

FIG. 12. Differential cross section in nb/sr for $^{13}C(\gamma,\pi^-)^{13}N_{g.s.}$ at $T_\pi=50$ MeV in the nonlocal DWIA calculation. The full line shows $E0+M1$ with the full BL operator, while the short- and long-dashed lines are obtained for $E0$ and $E0+M1$, respectively, both with the Δ excitation omitted. The preliminary data points are from Stoler *et al.* (Ref. 23).

operator gives a different energy distribution than the local calculation[20] but is about a factor of 5 bigger than the data points. Furthermore, the $E0$ contribution which has no nuclear structure uncertainties is already a factor of 4 too big. By removing the Δ contribution, however, the low cross section of the data could be explained. The same is true for the 65° data point of the new Amsterdam experiments.[23] Also here a theoretical explanation can be given by removing the Δ in the B-L operator (see Fig. 12). At this point one could speculate that the Δ excitation does not show up in γ,π reactions on nuclei at all. Toker and Tabakin[22] pointed out that including the Δ excitation in the production operator and in the optical potential may result in some double counting. We believe that the contribution of the Δ in the B-L operator is overestimated at low energy, but is probably right in the resonance region around 300 MeV. If we examine the result shown for $\gamma n \rightarrow \pi^- p$ in Fig. 10, we find that at 50 MeV pion energy the influence of the Δ is negligible in the elementary process as compared to the nuclear case $^{13}C(\gamma,\pi^-)^{13}N_{g.s.}$. To clarify this point an experiment done in the minimum region around $Q=1$ fm^{-1} which covers an energy range from well below to well above the resonance would be most desirable (see Fig. 9).

X. SUMMARY AND CONCLUSION

In this paper we have presented a momentum space calculation of pion photoproduction from p-shell nuclei. It is performed in the framework of a distorted wave impulse approximation with pion wave functions obtained from the optical potential of Stricker, McManus, and Carr[34] and the Blomqvist-Laget[33] amplitudes. Unlike coordinate space calculations our method is suitable for any analytic form of pion production operators and treats nonlocalities exactly. Since it is still an unsolved numerical problem to include the Coulomb distortions in momentum space, a limit to the validity of our calculations is given for the threshold region. However, a major purpose of this work is the Δ resonance region, where Coulomb effects can be neglected. Also around 50 MeV the effects of the Coulomb potential can be expected to be smaller than the current uncertainties of experiment and theory.

The main point of this work is a study of operator effects for pion photoproduction which is mainly independent of the nuclear structure of a specific transition. In this way our results on the partial cross sections are universal for any such reaction in the $1p$ shell for a large variety of ground states and low lying excited states. From a total of ten different transitions, determined by angular momentum L, spin S, and total spin J all γ,π reactions are given. Some reactions like $^{10}B(\gamma,\pi^-)^{10}C_{g.s.}$ involve only 1 transition, others like $^{13}C(\gamma,\pi^-)^{13}N_{g.s.}$ a total of six, and $^{11}B(\gamma,\pi^-)^{11}C_{g.s.}$ involves all ten of them. However, we found that from threshold up to energies well above the resonance a total of six transitions play a dominant role. In $E0$ transitions it is $\alpha=1$, with $L=0$, $S=0$, and $J=0$. This σ_{11} element is the most interesting one in respect to the Δ resonance excitation. Even at rather low energies of $T_\pi=50$ MeV the contribution of the Δ shows up significantly and taking the resonance into account and leaving it out results in a factor of more than 2 at pion angles between 40° and 90°. A comparison with a recent experiment on $^{13}C(\gamma,\pi^-)^{13}N_{g.s.}$ even suggests that the Δ is totally absent. From the study of the elementary reaction on the neutron we have seen that the total $S=0$ contribution at this energy is quite unimportant. From this point of view, the threshold behavior of the $S=0$ Δ excitation can be wrong in the Blomqvist-Laget approach. Another explanation can be the neglect of Δ-propagation effects which are only treated in Δ-hole calculations. From such calculations on γ,π^0 it is known that the Δ contribution is lowered,[43] but not by such a dramatic amount. To rule out a nuclear structure effect like core polarization, the best way to investigate this is an experimental study at the same kinematics for the reaction $^{15}N(\gamma,\pi^-)^{15}O_{g.s.}$ when the same nuclear transitions occur as in ^{13}C, but with different weights. Also, we have shown that a kinematical separation of the $E0$ can be obtained at $Q\approx 1$ fm^{-1} where the $M1$ cross section is minimal. In this case the Δ excitation enhances the cross section by a factor of 6. Finally there is one unique example for a pure $E0$ transition. This is $^{14}C(\gamma,\pi^-)^{14}N^*$ which leads to the first excited state in ^{14}N, the isospin analog of $^{14}C_{g.s.}$ and $^{14}O_{g.s.}$ (Ref. 44). If one can overcome the difficulties with the ^{14}C target this will be a unique experiment.

In $M1$ reactions there are two transitions $\alpha=4$, with $L=0$, $S=1$, and $J=1$ and $\alpha=6$ with $L=2$, $S=1$, and $J=1$, that play an important role. In general they can both become large and interfere strongly. Since the Q dependence of the reduced cross sections is roughly Q^L, the $\alpha=4$ dominates for small momentum transfer. Furthermore, this transition shows very little operator effects and is mainly given by the Kroll-Ruderman term. This situation changes for σ_{66}, which shows more operator sensitivity than σ_{44}. But these effects are far less pronounced than in monopole transitions. In most $M1$ transitions we get an interference between $\alpha=4$ and 6; however, in the 15.11 MeV transition of ^{12}C the reduced nuclear matrix element ψ_6 is small, so, apart from the minimum, the σ_{44} term can be singled out. And in the 2.31 MeV transition of ^{14}N the Gamow-Teller matrix element $\psi_4\simeq 0$, so here the σ_{66} term can be studied.

In $E2$ reactions there are also two dominant transitions possible, $\alpha=7$ with $L=2$, $S=0$, and $J=2$, and $\alpha=9$ with $L=2$, $S=1$, and $J=2$. Here the $\alpha=7$ is most interesting because it shows similar characteristics as $E0$, as it is dominated by Δ excitation. For isoelastic reactions like $^{11}B(\gamma,\pi^-)^{11}C_{g.s.}$, $\psi_9=0$ from time reversal symmetry, so apart from the small nonlocal contribution with $\alpha=8$ the $E2$ cross section is given by σ_{77}. However, in such reactions not only $E2$ but also $E0$, $M1$, and $M3$ are involved, therefore an $E2$ effect will be very hard to see. The situation is different in analog transitions. In $^{12}C(\gamma,\pi^+)^{12}B(2^+1;\ 0.95\ \text{MeV})$ a pure $E2$ transition can be studied, however, both $\alpha=7$ and 9 contribute equally well. Nevertheless the Δ should show up according to our analysis.

Finally there is only one $M3$ transition, $\alpha=10$ with $L=2$, $S=1$, and $J=3$ and a famous p-shell example,

$^{10}B(\gamma,\pi^+)^{10}Be_{g.s.}$ and $^{10}B(\gamma,\pi^-)^{10}C_{g.s.}$. Since there is no interference with different matrix elements and the fact that $\sigma_{10,10}$ is dominated by the Kroll-Ruderman term, even in the region of the Δ resonance only small operator effects will show up. This explains why even simple calculations were so successful in describing the experimental data.[6]

In conclusion, we find that this kind of analysis is quite useful for proposing future experiments of γ,π on light nuclei which can shed more light in the production process and may eventually be used in testing different nuclear models in a more complete way than standard elastic or inelastic electron scattering experiments. The development of continuous wave electron accelerators will very soon provide clean monochromatic photon beams and the accuracy of experimental data will improve very much. Experiments will also be performed to nuclear excitation levels which are not well enough separated for current techniques. Eventually coincidence experiments such as (e,e'π) will be performed, and with the combined information it should be possible to disentangle the three different aspects of pion production; nuclear structure, pion production from bound nucleons, and pion distortions by nuclei.

ACKNOWLEDGMENTS

We would like to thank Dr. A. M. Bernstein and Dr. P. Stoler for very useful discussions on this subject and Dr. M. Krell for providing us with his computer code for pion optical potentials. One of us (L.T.) wants to thank the TRIUMF Theory Group for the hospitality and for many inspirations during his stay at TRIUMF. This work was supported in part by the U.S. Department of Energy Contract DE-AC02-79ER10397-3, the Deutsche Forschungsgemeinschaft (SFB 201), and the Natural Sciences and Engineering Research Council of Canada.

APPENDIX: BLOMQVIST-LAGET AMPLITUDES IN SPIN DECOMPOSITION

The elementary pion photoproduction amplitudes for charged pions with charge β have the general form

$$t=(L+i\vec{\sigma}\cdot\vec{K})\frac{\tau-\beta}{\sqrt{2}}\ ,$$

where L and $\vec{K}$ are the spin 0 and spin 1 transition amplitudes, respectively. In the model of Blomqvist and Laget[33] these amplitudes are derived as a nonrelativistic reduction of covariant Feynman amplitudes for the first order Born terms and the s-channel $\Delta(1236)$ excitation. Choosing the pseudovector (PV) pion-nucleon coupling model we find the following spin decomposition for $\gamma p\to n\pi^+$:

$$L_{PV}=\frac{\sqrt{2}g_0}{2m}\left[\frac{\mu_p}{2E_a(P_a^0-E_a)}+\frac{\mu_n}{2E_b(P_b^0-E_b)}\right]\vec{q}\cdot(\vec{k}\times\vec{\epsilon})\ ,$$

$$\vec{K}_{PV}=\frac{\sqrt{2}g_0}{2m}\left\{\left[-1+\frac{mE_\pi}{E_a(P_a^0+E_a)}\right]\vec{\epsilon}+\left[\frac{\mu_p}{2E_a(P_a^0-E_a)}-\frac{\mu_n}{2E_b(P_b^0-E_b)}\right](\vec{k}\,\vec{\epsilon}\cdot\vec{q}-\vec{\epsilon}\,\vec{k}\cdot\vec{q})\right.$$
$$\left.+\frac{(\vec{k}-\vec{q})\vec{\epsilon}\cdot\vec{q}}{\vec{k}\cdot\vec{q}-kE_\pi}-\frac{\vec{q}\,\vec{\epsilon}\cdot\vec{p}}{E_a(P_a^0-E_a)}\right\},$$

and for $\gamma n\to p\pi^-$

$$L_{PV}=\frac{\sqrt{2}g_0}{2m}\left[\frac{\mu_n}{2E_a(P_a^0-E_a)}+\frac{\mu_p}{2E_b(P_b^0-E_b)}\right]\vec{q}\cdot(\vec{k}\times\vec{\epsilon})\ ,$$

$$\vec{K}_{PV}=\frac{\sqrt{2}g_0}{2m}\left\{\left[1+\frac{mE_\pi}{E_b(P_b^0+E_b)}\right]\vec{\epsilon}+\left[\frac{\mu_n}{2E_a(P_a^0-E_a)}-\frac{\mu_p}{2E_b(P_b^0-E_b)}\right](\vec{k}\,\vec{\epsilon}\cdot\vec{q}-\vec{\epsilon}\,\vec{k}\cdot\vec{q})\right.$$
$$\left.+\frac{(\vec{k}-\vec{q})\vec{\epsilon}\cdot\vec{q}}{\vec{k}\cdot\vec{q}-kE_\pi}-\frac{\vec{q}\,\vec{\epsilon}\cdot\vec{p}\,'}{E_b(P_b^0-E_b)}\right\}.$$

The photon, pion, incoming nucleon, and outgoing nucleon four-momenta are $(k,\vec{k})$, $(E_\pi,\vec{q})$, $(E,\vec{p})$, and $(E',\vec{p}\,')$, respectively; $\vec{\epsilon}$ is the polarization vector of the photon. The four-momenta in the s and u channels are $p_a^\mu=p^\mu+k^\mu$ and $p_b^\mu=p'^\mu-k^\mu$ and $E_{a,b}=(\vec{p}\,^2_{a,b}+m^2)^{1/2}$. The magnetic moments of the nucleons are $\mu_p=2.79$ and $\mu_n=-1.91$ nuclear magnetons and for the π-N coupling constant we choose $g_0^2/4\pi=14$.

For the s-channel $\Delta(1236)$ excitation we get for $\gamma,\pi^\pm$

$$L_\Delta = \pm \frac{2\sqrt{2}G_1G_3/9}{P_a^2 - m_\Delta^2 + i\Gamma m_\Delta} \left[\frac{E_\pi}{m} \vec{p}\cdot(\vec{k}\times\vec{\epsilon}) + \frac{m_\Delta - m}{m} \vec{q}\cdot(\vec{p}\times\vec{\epsilon}) - \vec{q}\cdot(\vec{k}\times\vec{\epsilon}) \right],$$

$$\vec{K}_\Delta = \pm \frac{\sqrt{2}G_1G_3/9}{P_a^2 - m_\Delta^2 + i\Gamma m_\Delta} \left\{ \left[-\vec{k}\cdot\vec{q} + \frac{E_\pi}{m_\Delta}(\vec{k}^2 + \vec{k}\cdot\vec{p}) + \frac{m_\Delta - m}{m}\vec{p}\cdot\vec{q} - \frac{E_\pi}{m_\Delta}\frac{m_\Delta - m}{m}(\vec{p}^2 + \vec{k}\cdot\vec{p}) \right] \vec{\epsilon} \right.$$

$$\left. + \left[\vec{\epsilon}\cdot\vec{q} - \frac{E_\pi}{m_\Delta}\vec{\epsilon}\cdot\vec{q} \right] \left[\vec{k} - \frac{m_\Delta - m}{m}\vec{p} \right] \right\}.$$

We have chosen the parametrization of Eq. (19) in Ref. 33 with the delta mass of $m_\Delta = 1231$ MeV. For the total amplitudes, the Born terms and the Δ excitation add coherently, so $L = L_{PV} + L_\Delta$ and $\vec{K} = \vec{K}_{PV} + \vec{K}_\Delta$.

---

*On leave from Universität Mainz, Mainz, Federal Republic of Germany.

[1] *Photopion Nuclear Physics,* edited by P. Stoler (Plenum, New York, 1979).

[2] M. K. Singham and F. Tabakin, Ann. Phys. (N.Y.) **135**, 71 (1981).

[3] A. M. Bernstein, in *Lectures at the International School of Intermediate Energy Nuclear Physics, Verona, 1981,* edited by R. Bergere, S. Costa, and C. Schaerf (World Scientific, Singapore, 1982).

[4] P. K. Teng *et al.*, Phys. Rev. C **26**, 1313 (1982).

[5] M. Yamazaki *et al.*, in *Proceedings of the Ninth International Conference on High Energy Physics and Nuclear Structure, Versailles, France, 1981,* edited by P. Catillon, P. Radvanyi, and M. Porneuf (North-Holland, Amsterdam, 1982), Vol. 115.

[6] B. W. Zukoskey, R. M. Sealock, H. S. Caplan, and J. C. Bergstrom, Phys. Rev. C **26**, 1610 (1982).

[7] D. Rowley *et al.*, Phys. Rev. C **25**, 2652 (1982).

[8] N. Paras *et al.*, Phys. Rev. Lett. **42**, 1455 (1979).

[9] N. Shoda, H. Ohashi, and K. Nakahara, Phys. Rev. Lett. **39**, 1131 (1977); Nucl. Phys. **A350**, 377 (1980).

[10] Ch. Schmitt *et al.*, Nucl. Phys. **A392**, 345 (1983).

[11] J. LeRose *et al.*, Phys. Rev. C **25**, 1702 (1982).

[12] J. LeRose *et al.*, Phys. Rev. C **26**, 2554 (1982).

[13] N. Shoda, O. Sasaki, and T. Nohmura, Phys. Lett. **101B**, 124 (1981).

[14] P. Bosted, K. I. Blomqvist, and A. M. Bernstein, Phys. Rev. Lett. **43**, 1473 (1979).

[15] L. Tiator and L. E. Wright, Nucl. Phys. **A379**, 407 (1982).

[16] A. Nagl and H. Uberall, Phys. Lett. **63B**, 291 (1976); **96B**, 254 (1980).

[17] M. K. Singham, G. N. Epstein, and F. Tabakin, Phys. Rev. Lett. **43**, 1478 (1978); G. N. Epstein, M. K. Singham, and F. Tabakin, Phys. Rev. C **17**, 702 (1978).

[18] N. Freed and P. Ostrander, Phys. Lett. **61B**, 449 (1976); V. DeCarlo and N. Freed, Phys. Rev. C **25**, 2162 (1982).

[19] V. Devanathan, V. Girija, and G. N. Prasad, Can. J. Phys. **58**, 1151 (1980).

[20] L. Tiator, Phys. Lett. **125B**, 367 (1983).

[21] S. Maleki, Nucl. Phys. **A403**, 607 (1983).

[22] G. Toker and F. Tabakin, Phys. Rev. C **28**, 1725 (1983).

[23] P. Stoler *et al.* (private communication).

[24] J. D. Bjorken and S. D. Drell, *Relativistic Quantum Mechanics* (McGraw-Hill, New York, 1964).

[25] T. W. Donnelly and W. C. Haxton, At. Data Nucl. Data Tables **23**, 103 (1979).

[26] S. Cohen and D. Kurath, Nucl. Phys. **73**, 1 (1965).

[27] N. Ensslin *et al.*, Phys. Rev. C **9**, 1705 (1974).

[28] J. M. Eisenberg and D. S. Koltun, *Theory of Meson Interactions with Nuclei* (Wiley, New York, 1980).

[29] L. Tiator, A. K. Rej, and D. Drechsel, Nucl. Phys. **A333**, 343 (1980).

[30] Program developed by M. Krell and A. W. Thomas from an earlier version from M. Krell and S. Barmo, Nucl. Phys. **B20**, 461 (1970).

[31] F. A. Berends, A. Donnachie, and D. L. Weaver, Nucl. Phys. **B4**, 1 (1967); **B4**, 54 (1967); **B4**, 103 (1967); F. A. Berends and D. L. Weaver, *ibid.* **B84**, 342 (1974).

[32] G. F. Chew, M. L. Goldberger, F. B. Low, and Y. Nambu, Phys. Rev. **106**, 1337 (1957); **106**, 1345 (1957).

[33] K. I. Blomqvist and J. M. Laget, Nucl. Phys. **A280**, 405 (1977).

[34] K. Stricker, H. McManus, and J. A. Carr, Phys. Rev. C **19**, 929 (1979).

[35] K. Stricker, J. A. Carr, and H. McManus, Phys. Rev. C **22**, 2043 (1980).

[36] J. A. Carr, H. McManus, and K. Stricker-Bauer, Phys. Rev. C **25**, 952 (1982).

[37] L. Tiator, Nucl. Phys. **A364**, 189 (1981).

[38] I.-T. Cheon, Z. Phys. A **306**, 353 (1982).

[39] K. Shoda *et al.*, Phys. Rev. C **27**, 443 (1983).

[40] T.-S. H. Lee and D. Kurath, Phys. Rev. C **21**, 293 (1980).

[41] R. S. Hicks *et al.*, Phys. Rev. C **26**, 339 (1982).

[42] M. Salomon *et al.*, Nucl. Phys. A (to be published).

[43] J. H. Koch and E. J. Moniz, Phys. Rev. C **27**, 751 (1983).

[44] A. M. Bernstein, L. Tiator, and L. E. Wright (unpublished).